Clutter simulation techniques

Introduction

In the previous session we discussed the modeling of non-Gaussian sea clutter and its effects on radar performance. The compound form of the K distribution proved to be particularly valuable; the classic, Gaussian noise, results were redeemed by integration over a gamma distribution of local power. Nonetheless there are many situations that are not amenable to direct analytic attack; this approach may not be the most revealing and convenient, even when it is possible. So, to complement the analytic approach of the previous session, we will look at the simulation of clutter returns; this provides us with another route along which we can approach radar performance problems. Our analytic models for clutter have been exclusively statistical; this prejudice is still evident in the simulation methods we look at. In essence we must confront the problem of generating correlated random numbers with prescribed one and two point statistics (i.e. PDF and correlation function.) In the case where the simulated process is Gaussian reasonable progress can be made; this provides us with both a good place to start and a valuable simulation tool. The controlled simulation of correlated non-Gaussian processes is much more difficult. Fortunately we are mainly interested in simulating clutter, for which the compound model has proved to be very effective; the Gaussian simulation techniques allow us to get at the 'speckle' component without too much difficulty. The principal difficulty we then encounter is in the simulation of the correlated variation in the local power component. Significant progress can be made towards the solution of this problem, adopting a fairly pragmatic, 'knife and fork', approach. Once we can simulate a gamma process in this way, we are able to generate K distributed clutter. When we have done this we will have a reasonable, physically motivated clutter simulation capability that should stand us in good stead for the solution of practical radar performance problems. Before we can do any of this, however, we consider the basic building block of all these simulation methods, the generation of un-correlated random numbers with a known (usually Gaussian) PDF.

Generating un-correlated random numbers with a prescribed PDF

Modern computers can readily supply us with a succession of un-correlated random numbers *x*, uniformly distributed between 0 and 1; this we take as our starting point, without further explanation. (In Mathematica **`Random[]`** does this for us. For the moment we will use *x* exclusively to denote this uniformly distributed random variable, later on we will doubtless use *x* for other things as well) These can be mapped onto a collection of un-correlated numbers *y* with a PDF $P_{\mathbf{y}}(y)$ by equating the cumulative distribution of each. Thus we have

$$P_{\mathbf{x}}(x) = 1, \quad 0 \le x < 1$$

$$C_{\mathbf{x}}(x) = \int_0^x P_{\mathbf{x}}(x')dx' = x = C_{\mathbf{y}}(y) = \int_{-\infty}^y P_{\mathbf{y}}(y')dy' \tag{1}$$

So, given the value *x* generated by the computer, we solve this equation for *y*, which now has the PDF $P_{\mathbf{y}}(y)$. This relationship is fundamentally important; we will return to it when we come to simulate correlated non-Gaussian processes. In some cases the transformation from *x* to *y* is relatively straightforward. Thus, if *y* is required to have an exponential distribution, we have

$$\begin{aligned} &P_{\mathbf{y}}(y) = \exp(-y), \quad y \ge 0 \\ &x = \int_0^y \exp(-y')dy' = 1 - \exp(-y) \\ &y = -\log(1-x) \end{aligned} \tag{2}$$

As 1-*x* and *x* have the same distribution we can also write this transformation between uniformly and exponentially distributed random numbers as $y = -\log(x)$. The generation of un-correlated Gaussian random numbers is particularly important in practical applications. At first sight we might think that we must solve

$$x = \frac{1}{\sqrt{\pi}} \int_{-\infty}^{y} \exp\left(-y'^2\right) dy' = \frac{1}{2} + \mathrm{erf}(y) \tag{3}$$

at each step in the simulation; fortunately this can be avoided by the following trick. Consider two independent Gaussian random variables, y_1, y_2 with the joint PDF

$$P_{\mathbf{y}_1\mathbf{y}_2}(y_1, y_2) = \frac{1}{\pi} \exp\left(-y_1^2 - y_2^2\right) \tag{4}$$

If we now represent these in polar form

$$y_1 = r\cos\theta, \quad y_2 = r\sin\theta \tag{5}$$

then the joint PDF of these polar variables is

$$\begin{aligned} &P_{\mathbf{r}\boldsymbol{\theta}}(r,\theta) = P_{\mathbf{r}}(r) P_{\boldsymbol{\theta}}(\theta); \\ &P_{\mathbf{r}}(r) = 2r\exp\left(-r^2\right), \quad P_{\boldsymbol{\theta}}(\theta) = \frac{1}{2\pi} \end{aligned} \tag{6}$$

Thus the polar angle is uniformly distributed, and so can be simulated through

$$\theta = 2\pi x_1 \tag{7}$$

We also see that r^2 is exponentially distributed; thus *r* can be simulated through

$$r = \sqrt{-\log(x_2)}\,. \tag{8}$$

Thus, having generated two independent uniformly distributed random numbers x_1, x_2, we produce two independent Gaussian random variables y_1, y_2 as

$$y_1 = \sqrt{-\log(x_2)}\cos(2\pi x_1), \quad y_2 = \sqrt{-\log(x_2)}\sin(2\pi x_1). \tag{9}$$

We note that these *y* variables each has a zero mean and a variance of $1/2$; a Gaussian random variable with a mean of μ and a variance of σ^2 is obtained when we then form $\mu + \sqrt{2\sigma^2}\,y$. A Gaussian random variable with zero mean and unit variance is required in many of our simulations, we denote it by *g*.

Independent random variables with other PDFs can be generated similarly; considerable cunning has been deployed in the efficient solution of (1). Mathematica (and other) software packages implement many of these as built in functions; should you need to generate independent non-Gaussian random variables for any reason you should always see if the hard work has been done for you already.

Generating correlated Gaussian random numbers

We recall that the sum of two Gaussian random variables itself has Gaussian statistics; subjecting a Gaussian process to any linear operation (e.g. filtering, integration or differentiation) similarly yields another Gaussian process. The qualitative effects of the linear operation are manifest in the correlation properties of the output process, rather than in its single point statistics. A simple, and practically useful, simulation of a correlated Gaussian process is as follows. Consider the simple recurrence (or feedback)

$$x_n = \eta x_{n-1} + \beta g_n \ . \tag{10}$$

The g are zero mean, unit variance independent Gaussian radnom numbers; η is chosen to have magnitude less than 1 to keep things stable. If we start things of with n =0 we can write the solution to (10) as

$$x_n = \eta^n x_0 + \beta \sum_{r=0}^{n-1} \eta^r g_{n-r} \tag{11}$$

Apart from the transient term, this can be viewed as the output of a filter acting on the succession (or time series) of gs. The mean value of x_n, averaged over realisations of the gs consists of the transient term

$$\langle x_n \rangle = \eta^n x_0 + \beta \sum_{r=0}^{n-1} \eta^r \langle g_{n-r} \rangle = \eta^n x_0 \tag{12}$$

while its mean square is

$$\begin{aligned} \langle x_n^2 \rangle &= \eta^{2n} x_0^2 + \beta^2 \sum_{r,s=0}^{n-1} \eta^{r+s} \langle g_{n-r} g_{n-s} \rangle \\ &= \eta^{2n} x_0^2 + \beta^2 \sum_{r=0}^{n-1} \eta^{2r} \\ &= \eta^{2n} x_0^2 + \frac{\beta^2 \left(1 - \eta^{2n}\right)}{1 - \eta^2} \end{aligned} \tag{13}$$

Once the transient terms have died down, we see that the output of the process is a zero mean Gaussian process with a modified variance. More importantly, however, correlation has been induced in this output, that was absent in the succession of un-correlated gs that serve as its input. This correlation can be calculated directly

$$
\begin{aligned}
x_n &= \eta^n x_0 + \beta \sum_{r=1}^{n} \eta^{n-r} g_r; \quad x_{n+m} = \eta^{n+m} x_0 + \beta \sum_{r=1}^{n+m} \eta^{n+m-r} g_r \\
\langle x_n x_{n+m} \rangle &= \eta^{2n+m} x_0 + \beta^2 \sum_{r=1}^{n+m} \sum_{s=1}^{n} \eta^{2n+m-r-s} \langle g_r g_s \rangle \\
&= \eta^{2n+m} x_0 + \beta^2 \sum_{s=1}^{n} \eta^{2n+m-2s} \\
&= \eta^m \langle x_n^2 \rangle
\end{aligned}
\tag{14}
$$

Thus we see how the linear feedback process has induced a correlation in the output Gaussian process, that we can control through the parameter η; β allows us to control the power of the output process. If we chose

$$\beta = \sqrt{1-\eta^2} \tag{15}$$

we ensure that the output has a unit variance, once transients have died down. A simple correlated Gaussian generated in this way can itself be a very useful simulation tool.

We see from (11) that this method provides an example of the use of a filter to induce correlation in a Gaussian process; this in turn relates directly to the description of the output process in terms of its power spectrum. It is interesting to see how this approach is intimately related to the stochastic differential equation description of random processes. We recall the Ornstein –Uhlenbeck process (over damped Brownian harmonic oscillator), evolving subject to the Langevin equation

$$\frac{dx(t)}{dt} = -\alpha x(t) + f(t) \tag{16}$$

Here *f* is white noise for which

$$\langle f(t) f(t') \rangle = 2\alpha\delta(t-t') \tag{17}$$

We integrate this up, formally at least, to give us something very similar to (10)

$$x(t) = \exp(-\alpha t) x(0) + \int_0^t \exp(-\alpha(t-t_1)) f(t_1) dt_1 \tag{18}$$

Thus, if we propagate the process over the time-step between t_{n-1} and t_n and compare (10) with (18) we can make the identifications

$$
\begin{aligned}
&\eta = \exp(-\alpha(t_n - t_{n-1})) \\
&\beta g_n = \int_{t_{n-1}}^{t_n} \exp(-\alpha(t_n - t)) f(t) dt \\
&\langle g_n \rangle = 0 \\
&\beta^2 = \int_{t_{n-1}}^{t_n} \int_{t_{n-1}}^{t_n} dt_1 dt_2 \exp(-\alpha(2t_n - t_1 - t_2)) \langle f(t_1) f(t_2) \rangle = (1-\eta^2)
\end{aligned}
\tag{19}
$$

We can also regard the first term in (18) as a transient; at long times, when such effects have settled down, we have

$$\begin{aligned}\left\langle x^2 \right\rangle &= \int_0^\infty dt_1 \int_0^\infty dt_2 \exp\left(-\alpha\left(2t - t_1 - t_2\right)\right)\left\langle f\left(t_1\right) f\left(t_2\right)\right\rangle \\ \left\langle x^2 \right\rangle &= 1\end{aligned} \tag{20}$$

(17) embodies a simple 'fluctuation-dissipation' result, which requires the input white noise (fluctuation) and the linear resistance (dissipation) terms to balance out to establish an equilibrium mean square value. The power spectrum of the process can be derived from either (19) or the underlying SDE as

$$S\left(\omega\right) = \frac{2\alpha}{\alpha^2 + \omega^2} \tag{21}$$

A simple generalisation of the OU process that is particularly useful in clutter modeling is its complex version; the anologue of (10)

$$z_n = \exp\left(-\left(\alpha/2 + i\omega_0\right)\left(t_n - t_{n-1}\right)\right) z_{n-1} + \sqrt{\frac{\left(1 - \exp\left(-\alpha\left(t_n - t_{n-1}\right)\right)\right)}{2}}\left(g_{In} + i g_{Qn}\right) \tag{22}$$

This generates a complex Gaussian process, with a characteristic 'Doppler' frequency ω_0, with a unit mean power and an exponentially decaying intensity acf. Realisations of this process cropped up in the Fourier analysis session; we recall that they looked sufficiently 'lifelike' to be mistaken for samples of real data.

Higher dimensional Gaussian processes

Going for the multi-dimensional case we adopt a vector notation and set up the Langevin equation as

$$\frac{d\mathbf{x}\left(t\right)}{dt} = \mathbf{A} \cdot \mathbf{x}\left(t\right) + \mathbf{f}\left(t\right) \tag{23}$$

The matrix **A** is constant; to ensure that the system is stable all its eigenvalues must be negative (in the real part). Once again we integrate it up formally

$$\mathbf{x}\left(t\right) = \exp\left(\mathbf{A}t\right)\mathbf{x}\left(0\right) + \int_0^t \exp\left(\mathbf{A}\left(t - t_1\right)\right) \cdot \mathbf{f}\left(t_1\right) dt_1 \tag{24}$$

The white noise vector **f** has a correlation matrix of the form (which we don't know yet)

$$\left\langle \mathbf{f}\left(t_1\right)\mathbf{f}\left(t_2\right)^T \right\rangle = \delta\left(t_1 - t_2\right)\mathbf{G} \tag{25}$$

In the long time limit, where all the transients have died down, we can construct the covariance matrix **B** of **x**, just as we did in (3) above

$$\begin{aligned}\left\langle \mathbf{x}\mathbf{x}^T \right\rangle &= \lim_{t\to\infty} \int_0^t dt_1 \int_0^t dt_2 \exp(\mathbf{A}(t-t_1))\mathbf{G}\exp\left(\mathbf{A}^T(t-t_2)\right)\delta(t_1-t_2) \\ &= \int_0^\infty dt \exp(\mathbf{A}t)\mathbf{G}\exp\left(\mathbf{A}^T t\right) \\ &= \mathbf{B}\end{aligned} \tag{26}$$

A quick integration by parts tell us that

$$\mathbf{A}\mathbf{B} + \mathbf{B}\mathbf{A}^T = \int_0^\infty dt \frac{d\left(\exp(\mathbf{A}t)\mathbf{G}\exp\left(\mathbf{A}^T t\right)\right)}{dt} = -\mathbf{G} \tag{27}$$

This is neat; it tells us, once we have prescribed our equilibrium statistics **B** and the relaxation processes **A**, the way in which we must drive the Langevin equations in order to maintain these. Thus given the dissipation, we can identify the fluctuations consistent with the prescribed covariance. Should the matrix **G** have any negative eigenvalues, presumably you are asking for a system that cannot be realised (it would have a negative power spectrum.) To implement this as a simulation we can discretise the evolution equation as

$$\begin{aligned}&\mathbf{x}_n = \mathbf{H}\cdot\mathbf{x}_{n-1} + \mathbf{V}_n \\ &\mathbf{H} = \exp(\mathbf{A}(t_n - t_{n-1})) \\ &\left\langle \mathbf{V}_n \right\rangle = \mathbf{0} \\ &\left\langle \mathbf{V}_n \mathbf{V}_n^T \right\rangle = \int_0^{t_n - t_{n-1}} \exp(\mathbf{A}t)\cdot\mathbf{G}\cdot\exp\left(\mathbf{A}^T t\right)dt\end{aligned} \tag{28}$$

We now substitute our expression for **G**, whereupon everything sorts itself out very nicely

$$\begin{aligned}\left\langle \mathbf{V}_n \mathbf{V}_n^T \right\rangle &= -\int_0^{t_n - t_{n-1}} \exp(\mathbf{A}t)\left(\mathbf{A}\cdot\mathbf{B} + \mathbf{B}\cdot\mathbf{A}^T\right)\exp\left(\mathbf{A}^T t\right)dt \\ &= -\int_0^{t_n - t_{n-1}} \frac{d\left(\exp(\mathbf{A}t)\cdot\mathbf{B}\cdot\exp\left(\mathbf{A}^T t\right)\right)}{dt} \\ &= \mathbf{B} - \mathbf{H}\cdot\mathbf{B}\cdot\mathbf{H}^T\end{aligned} \tag{29}$$

It is reassuring to note that this result ties in with the following, rather slapdash, analysis:

$$\begin{aligned}
&\mathbf{V}_n = \mathbf{x}_n - \mathbf{H}\cdot\mathbf{x}_{n-1}; \quad \mathbf{V}_n\mathbf{V}_n^T = \left(\mathbf{x}_n - \mathbf{H}\cdot\mathbf{x}_{n-1}\right)\left(\mathbf{x}_n - \mathbf{H}\cdot\mathbf{x}_{n-1}\right)^T \\
&\left\langle \mathbf{V}_n\mathbf{V}_n^T \right\rangle = \left\langle \mathbf{x}_n\mathbf{x}_n^T \right\rangle - \mathbf{H}\cdot\left\langle \mathbf{x}_{n-1}\mathbf{x}_n^T \right\rangle - \left\langle \mathbf{x}_n\mathbf{x}_{n-1}^T \right\rangle\cdot\mathbf{H}^T + \mathbf{H}\cdot\left\langle \mathbf{x}_{n-1}\mathbf{x}_{n-1}^T \right\rangle\cdot\mathbf{H}^T \\
&\left\langle \mathbf{x}_n\mathbf{x}_n^T \right\rangle = \left\langle \mathbf{x}_{n-1}\mathbf{x}_{n-1}^T \right\rangle = \mathbf{B} \\
&\left\langle \mathbf{x}_{n-1}\mathbf{x}_n^T \right\rangle = \mathbf{B}\cdot\mathbf{H}^T, \quad \left\langle \mathbf{x}_n\mathbf{x}_{n-1}^T \right\rangle = \mathbf{H}\cdot\mathbf{B} \\
&\left\langle \mathbf{V}_n\mathbf{V}_n^T \right\rangle = \mathbf{B} - \mathbf{H}\cdot\mathbf{B}\cdot\mathbf{H}^T
\end{aligned} \tag{30}$$

The matrix notation we have used here does rather conceal some of the complexity of the algebra involved. The under-damped Brownian harmonic oscillator, which formed the substance of one of the exercises for Session 6, is a relatively simple example. We can identify the matrix **A** as

$$\mathbf{A} = \begin{pmatrix} 0 & 1 \\ -\omega_0^2 & -\zeta/m \end{pmatrix} \tag{31}$$

while the equilibrium covariance matrix of the position and velocity variables is formed from the thermal averages

$$\mathbf{B} = \begin{pmatrix} kT/m\omega_0^2 & 0 \\ 0 & kT/m \end{pmatrix}. \tag{32}$$

Substituting these results into (27) we find the correlation matrix of the white noise driving terms required to establish these equilibrium values is given by

$$\mathbf{G} = \begin{pmatrix} 0 & 0 \\ 0 & 2kT\zeta/m^2 \end{pmatrix} \tag{33}$$

Now we consider a real life problem, the simulation of a Gaussian process with four characteristic relaxation times, used to model the aircraft motions, in a little more detail. In this application the power spectrum of the aircraft's displacement from its navigated path is prescribed as

$$S(\omega) = \frac{1}{\prod_{k=1}^{4}\left(1 + \omega^2/\omega_k^2\right)} \tag{34}$$

We have already seen that Fourier transformation of the Langevin equation leads us rapidly to the power spectrum of the process. This leads us to consider the following set of coupled differential equations:

$$\begin{aligned}
\frac{dx_1}{dt} &= x_2 \\
\frac{dx_2}{dt} &= x_3 \\
\frac{dx_3}{dt} &= x_4 \\
\frac{dx_4}{dt} &= -\sigma_4 x_1 - \sigma_3 x_2 - \sigma_2 x_3 - \sigma_1 x_4 + f(t)
\end{aligned} \tag{35}$$

Expressed only in terms of x_1 this gives us

$$\frac{d^4x_1}{dt^4}+\sigma_1\frac{d^3x_1}{dt^3}+\sigma_2\frac{d^2x_1}{dt^2}+\sigma_3\frac{dx_1}{dt}+\sigma_4x_1=f(t) \tag{36}$$

Fourier transformation then gives us

$$\left(\omega^4-i\omega^3\sigma_1-\omega^2\sigma_2+i\omega\sigma_3+\sigma_4\right)\tilde{x}_1(\omega)=\tilde{f}(\omega) \tag{37}$$

This can be written in the form

$$(i\omega-\omega_1)(i\omega-\omega_2)(i\omega-\omega_3)(i\omega-\omega_4)\tilde{x}_1(\omega)=\tilde{f}(\omega) \tag{38}$$

when we make the identifications

$$\begin{aligned}\sigma_1&=\omega_1+\omega_2+\omega_3+\omega_4\\ \sigma_2&=\omega_1\omega_2+\omega_1\omega_3+\omega_1\omega_4+\omega_2\omega_3+\omega_2\omega_4+\omega_3\omega_4\\ \sigma_3&=\omega_1\omega_2\omega_3+\omega_1\omega_2\omega_4+\omega_2\omega_3\omega_4+\omega_1\omega_3\omega_4\\ \sigma_4&=\omega_1\omega_2\omega_3\omega_4\end{aligned} \tag{39}$$

It follows that the spectrum of the process x_1 is

$$S_{11}(\omega)=\frac{S_{ff}(\omega)}{\left(\omega^2+\omega_1^2\right)\left(\omega^2+\omega_2^2\right)\left(\omega^2+\omega_3^2\right)\left(\omega^2+\omega_4^2\right)} \tag{40}$$

Thus the x_1 process has a spectrum of the hoped for form. (x_2, x_3 can be identified as the plane's velocity and acceleration.) To propagate this thing on the computer we draw on the results we have just derived; we know **A** and **G** and so must construct **H** and the variance of $\mathbf{V}_n$. **A** can be written in the form

$$\mathbf{A}=\mathbf{M}\cdot\mathbf{\Omega}\cdot\mathbf{M}^{-1}$$

$$\mathbf{\Omega}=\begin{pmatrix}-\omega_1&0&0&0\\0&-\omega_2&0&0\\0&0&-\omega_3&0\\0&0&0&-\omega_4\end{pmatrix}\quad\mathbf{M}=\begin{pmatrix}1&1&1&1\\-\omega_1&-\omega_2&-\omega_3&-\omega_4\\\omega_1^2&\omega_2^2&\omega_3^2&\omega_4^2\\-\omega_1^3&-\omega_2^3&-\omega_3^3&-\omega_4^3\end{pmatrix} \tag{41}$$

(which seems here to have been plucked out of thin air; see A.C. Aitken 'Determinants and Matrices', Oliver and Boyd, 1964, pp135-6, for a brief discussion of background material.) This allows us to write the matrix with which to form the transient part of the propagating solution as

$$\exp(\mathbf{A}t)=\mathbf{M}\cdot\exp(\mathbf{\Omega}t)\cdot\mathbf{M}^{-1} \tag{42}$$

Inspection of the coupled differential equations (36) tells us that

$$\mathbf{G} = \begin{pmatrix} 0 & 0 & 0 & 0 \\ 0 & 0 & 0 & 0 \\ 0 & 0 & 0 & 0 \\ 0 & 0 & 0 & 1 \end{pmatrix}; \quad G_{ij} = \delta_{i,4}\delta_{j,4} \tag{43}$$

(Alternatively one can identify the matrix **A** associated with the coupled differential equations (36) and evaluate **B**, the equilibrium covariance matrix of x_1, x_2, x_3, x_4, from the power spectrum (34). If one then expresses $\sigma_1, \sigma_2, \sigma_3, \sigma_4$ in terms of $\omega_1, \omega_2, \omega_3, \omega_4$ and forms the matrix $\mathbf{AB} + \mathbf{BA}^T$ one finds that all elements vanish except for 4,4. While it's nice to demonstrate this consistency, it would be overwhelmingly tedious and time consuming to carry through such an analysis if one did not have Mathematica to take the strain. You might like to work through this set of calculations, as much as an exercise in the use of Mathematica as anything else.)

We now calculate the variance of the random increment in **x**:

$$\begin{aligned} \left\langle \mathbf{V}_n \mathbf{V}_n^T \right\rangle &= \int_0^{\tau_n} \exp(\mathbf{A}t) \cdot \mathbf{G} \cdot \exp\left(\mathbf{A}^T t\right) dt; \quad \tau_n = t_n - t_{n-1} \\ &= \mathbf{M} \cdot \int_0^{\tau_n} \exp(\mathbf{\Omega} t) \cdot \mathbf{M}^{-1} \cdot \mathbf{G} \cdot \left(\mathbf{M}^{-1}\right)^T \cdot \exp(\mathbf{\Omega} t) dt \cdot \mathbf{M}^T \end{aligned} \tag{44}$$

Now

$$\left(\mathbf{M}^{-1} \cdot \mathbf{G} \cdot \left(\mathbf{M}^{-1}\right)^T \right)_{i,j} = \left(\mathbf{M}^{-1}\right)_{i4} \left(\mathbf{M}^{-1}\right)_{j4} \tag{45}$$

Direct evaluation of the matrix inverse tells us that (using Mathematica)

$$\left(\mathbf{M}^{-1}\right)_{k4} = -\frac{1}{\prod_{l \neq k} (\omega_k - \omega_l)} \tag{46}$$

Plugging this in gives us

$$\begin{aligned} &\left\langle \mathbf{V}_n \mathbf{V}_n^T \right\rangle = \mathbf{M} \cdot \mathbf{\Psi} \cdot \mathbf{M}^T \\ &(\mathbf{\Psi})_{ij} = \int_0^{\tau_n} \exp(-\omega_i t) \left(\mathbf{M}^{-1}\right)_{i4} \left(\mathbf{M}^{-1}\right)_{j4} \exp(-\omega_j t) dt = \frac{\left(1 - \exp\left(-\left(\omega_i + \omega_j\right)\tau_n\right)\right)}{\omega_i + \omega_j} \left(\mathbf{M}^{-1}\right)_{i4} \left(\mathbf{M}^{-1}\right)_{j4} \end{aligned} \tag{47}$$

(You might like to check that the long time limits of these results tie up with the covariance matrix obtained directly from the power spectrum (34); once again Mathematica makes the calculation feasible.) This covariance matrix is symmetric and positive definite and so can be factorised into the product of a matrix and its transpose, the so-called Cholesky decomposition. So, once we have evaluated $\left\langle \mathbf{V}_n \mathbf{V}_n^T \right\rangle$ we can perform this decomposition numerically:

$$\left\langle \mathbf{V}_n \mathbf{V}_n^T \right\rangle = \mathbf{P}\mathbf{P}^T \tag{48}$$

then generate a realisation of $\mathbf{V}_n$ as

$$\mathbf{V}_n = \mathbf{P} \cdot \mathbf{g}_n \tag{49}$$

where $\mathbf{g}_n$ is a vector of zero mean, unit variance, un-correlated Gaussian random numbers. This allows us to propagate the process as in (28).

Fourier synthesis of random processes.

We have already seen how the correlated sequence of Gaussian random numbers generated by feedback can be viewed as the output of a simple (one-pole, infinite response) filter. We will now look at how this approach might be extended. Consider the application of a filter to a white noise process *f*, to give the signal $\phi(t)$

$$\phi(t) = \int_{-\infty}^{\infty} h(t-t')f(t')dt' \tag{50}$$

We can evaluate the correlation function of this process as

$$\langle \phi(t)\phi(\tau+t) \rangle = \int_{-\infty}^{\infty} dt_1 \int_{-\infty}^{\infty} dt_2 h(t-t_1)h(t+\tau-t_2)\langle f(t_1)f(t_2) \rangle = \int_{-\infty}^{\infty} dt_1 h(t-t_1)h(t+\tau-t_1) \tag{51}$$

Alternatively we can Fourier transform the output of the filter to give us

$$\tilde{\phi}(\omega) = \tilde{h}(\omega)\tilde{f}(\omega) \tag{52}$$

and obtain its power spectrum as

$$S_{\phi\phi}(\omega) = \left|\tilde{h}(\omega)\right|^2 S_{ff}(\omega) \tag{53}$$

Thus we can relate the autocorrelation function and power spectrum of the output process to the filter function *h*. This relationship is not unique, as the phase of the filter function is not determined. Thus, for example we might identify the positive root of the power spectrum with the FT of the filter function

$$\tilde{h}(\omega) = \sqrt{S_{\phi\phi}(\omega)}; \tag{54}$$

One can then reconstruct the process $\phi(t)$ by Fourier inversion. In practice this is done discretely, using a FFT type algorithm, which in effect is evaluating a Fourier series (rather than a transform). Thus we consider a representation of the Gaussian process of the form

$$\phi(t) = \frac{a_0}{2} + \sum_{n=1}^{\infty}\left(a_n \cos\frac{2\pi nt}{T} + b_n \sin\frac{2\pi nt}{T}\right) \tag{55}$$

over a period of length *T*. The quantities a_n, b_n are independent zero mean Gaussian random variables with a variance given by the power spectrum of the process to be simulated, i.e.

$$\left\langle a_n^2 \right\rangle = \left\langle b_n^2 \right\rangle = S\left(\frac{2\pi n}{T}\right)\frac{2\pi}{T} \tag{56}$$

If now we wish to realise a sequence of *N* values of the random variable ϕ we can obtain this by taking the real part of the output of the FFT formed as

$$\phi(m\Delta) = \sum_{n=0}^{N-1}\sqrt{S\left(\frac{2\pi mn}{N\Delta}\right)\frac{2\pi}{\Delta}}\exp\left(-i\frac{2\pi nm}{N}\right)\left(g_{In} + ig_{Qn}\right) . \tag{57}$$

The Fourier synthesis method has two advantages over the real time simulation method, in that it can model correlation functions that cannot be expressed as a sum of exponentially decaying and oscillating terms, and can be extended to the simulation of random fields as well as of time series. Its principal disadvantage is that it produces samples in batches, rather than one at a time.

Approximate methods for the generation of correlated gamma distributed random numbers.

A random variable y is said to be gamma distributed if the pdf of its values *y* takes the form

$$\begin{aligned} P_\gamma(y) &= \frac{b^\nu}{\Gamma(\nu)} y^{\nu-1}\exp(-by) \quad y \geq 0 \\ &= 0 \quad y < 0 ; \end{aligned} \tag{58}$$

b and ν are referred to as the scale and shape parameters respectively. Much as in the one dimensional Gaussian case, the correlation function

$$\left\langle y(0)y(t)\right\rangle = \left\langle y^2\right\rangle R_\gamma(t) \tag{59}$$

can be defined. The form of this correlation function and the requirement that the marginal distributions of $y(0)$ and $y(t)$ have the form (58) are not sufficient to specify their joint pdf uniquely. Furthermore, a linear transformation of a gamma distributed process need not generate a process that itself has gamma single point statistics; this is a consequence of the gamma distribution's property of infinite divisibility, which contrasts with the stability of the Gaussian distribution. As a result the computer generation of a gamma process with a specified correlation function is less straightforward than the corresponding Gaussian simulation.

One approach to this problem was developed in the SAR group by Oliver and co-workers. In this an array of uncorrelated gamma variates $y_{\gamma,j}$ is generated, then weighted to induce the required correlation

$$y_{\Gamma,i} = \sum_{j=1}^{N} w_{ik} y_{\gamma,k} . \tag{60}$$

Unfortunately the higher order moments of $y_{\Gamma,i}$, which can be characterised in terms of those of $y_{\gamma,j}$ and the weights w_{ik}, are not consistent with a gamma distribution. Furthermore, fundamental restrictions are placed on the correlation properties that can be modeled in this way; in particular it is

not able to generate a correlation function that takes values less than the totally decorrelated value $\langle y \rangle^2$ Nonetheless this method is widely used and has been discussed extensively in the literature.

An alternative approach to the simulation of a correlated gamma process takes a correlated Gaussian process of zero mean and unit variance as its starting point. This is then mapped onto a gamma process *y* by the memoryless non-linear transform (MNLT) generated by the solution of the equation

$$\frac{1}{\sqrt{2\pi}}\int_x^\infty \exp\left(-x'^2/2\right)dx' = \frac{1}{\Gamma(\nu)}\int_y^\infty y'^{\nu-1}\exp(-y')\,dy' . \tag{61}$$

Used in conjunction with standard methods for generating Gaussian time series and random fields with prescribed correlation properties, this method can generate correlated time series and random fields that exhibit gamma single point statistics. For a long time it was thought that this MNLT puts forth a gamma variate whose correlation properties cannot be related in a simple and invertible way to those of the input Gaussian process. Consequently an empirical element has entered into the modeling of the correlation in the output gamma process. For example, it has been found that a Gaussian process with an exponentially decaying acf is transformed by the MNLT into a gamma process whose acf also displays a seemingly exponential decay over several decades. The following formula has been devised to relate the observed characteristic decay times of the Gaussian(τ_G) and gamma (τ_γ) processes and the ν parameter of the gamma distribution.

$$\frac{\tau_G}{\tau_\gamma} = 1 + \frac{0.15}{\nu^{0.7}} . \tag{62}$$

Empirical studies of the correlation properties of gamma processes derived from input Gaussian processes with Gaussian and power-law correlation functions have revealed the same apparent invariance in functional form of the corrrelation function under the MNLT and rules of thumb analogous to (62) have been devised that encapsulate the results of these numerical studies.

The generation of a correlated non-Gaussian process by MNTL

The MNLT method discussed in the previous section can be adapted to the general non-Gaussian case. The required MNLT or point non-linear transformation is defined by equating the cumulative distribution of a zero mean unit variance Gaussian process, evaluated at the value *x* taken by this process, with the cumulative distribution of the required process, thus determining the latter's value η. So, if the pdf of the values η of is $P_{\text{dist}}(\eta)$, we set

$$\int_\eta^\infty P_{\text{dist}}(\eta')d\eta' = \frac{1}{\sqrt{2\pi}}\int_x^\infty \exp\left(-x'^2/2\right)dx' = \frac{1}{2}\text{erfc}\left(x/\sqrt{2}\right) \tag{63}$$

where, in the second equality, we have identified the complementary error function. The complementary quantile function $Q_{\text{dist}}(\varsigma)$ of the required distribution is now defined by

$$\int_{Q_{\text{dist}}(\varsigma)}^{\infty} P_{\text{dist}}(\eta)d\eta = \varsigma\,; \tag{64}$$

using this we can write the MNLT that takes the input Gaussian random values into the corresponding values of the required non-Gaussian random variable as

$$\eta(x) = Q_{\text{dist}}\left(\text{erfc}\left(\text{x}/\sqrt{2}\right)/2\right). \tag{65}$$

The construction of this mapping is in general a non-trivial undertaking. The software package *Mathematica* supplies 'built in' quantile functions for a wide variety of non-Gaussian processes; these are, however rather slow in execution. A rapidly evaluable representation of (65) is a prerequisite if the MNLT approach is to be practically feasible.

We next evaluate the correlation function of the process η. This can be expressed in the form

$$\langle \eta(0)\eta(t)\rangle = \int_{-\infty}^{\infty} dx_1 \int_{-\infty}^{\infty} dx_2\ \eta(x_1)\eta(x_2)P_G\left(x_1, x_2, R_G(t)\right). \tag{66}$$

where

$$P_G\left(x(0), x(t), R_G(t)\right) = \frac{1}{2\pi\sqrt{1-R_G(t)^2}}\exp\left(-\left(x(0)^2 + x(t)^2 - 2x(0)x(t)R_G(t)\right)\Big/2\left(1-R_G(t)^2\right)\right) \tag{67}$$

The two dimensional integration implicit in (66) can be avoided by recalling the expansion discussed in session 5

$$P_G\left(x_1, x_2, R_G(t)\right) = \frac{\exp\left(-\left({x_1}^2 + {x_2}^2\right)/2\right)}{2\pi}\sum_{n=0}^{\infty}\frac{H_n\left(x_1/\sqrt{2}\right)H_n\left(x_2/\sqrt{2}\right)}{2^n n!}R_G(t)^n \tag{68}$$

where the H_n are Hermite polynomials defined by

$$H_n(z) = (-1)^n \exp\left(z^2\right)\frac{d^n}{dz^n}\exp\left(-z^2\right). \tag{69}$$

(68) provides us with an expansion of the propagator of the Ornstein-Uhlenbeck process in terms of eigenfunctions of its associated Fokker-Planck equation; the Hermite polynomials effectively encode the factorisation properties of the correlation functions of the Gaussian process. This expansion of the joint pdf as a power series in the input correlation function leads to a representation of the output correlation function that is computationally useful and highlights the extent to which the latter is modified relative to the former.

Using (68) we find that

$$\langle \eta(0)\eta(t)\rangle = \frac{1}{\pi}\sum_{n=0}^{\infty}\frac{R_G(t)^n}{2^n n!}\left(\int_{-\infty}^{\infty} dx \exp\left(-x^2\right)H_n(x)Q_{\text{dist}}\left(\text{erfc}(\text{x})/2\right)\right)^2. \tag{70}$$

Once we have evaluated the integrals

$$\int_{-\infty}^{\infty} dx \exp\left(-x^2\right) H_n(x) Q_{\text{dist}}\left(\text{erfc}(\text{x})/2\right) \tag{71}$$

we have a power series representation of the mapping between the correlation functions of the input Gaussian and output non-Gaussian processes. This series is rapidly convergent, or analytically summable, in most cases of interest. In particular we note that, when the series (70) contains only two non-negligible terms, it reduces to

$$\left\langle \eta(0)\eta(t)\right\rangle \approx \left\langle \eta\right\rangle^2 + \left(\left\langle \eta^2\right\rangle - \left\langle \eta\right\rangle^2\right) R_G(t) \tag{72}$$

and the correlation functions of the input and output processes are essentially identical. In general the higher order terms in (15) characterise the distortion in the correlation function induced by the MNLT that we sought to capture in the empirically derived rules of thumb used in approximate simulations.

So far, we have established a readily evaluable and invertible mapping between the correlation functions of the input Gaussian and output non-Gaussian processes related by the non-linear transformation (65). Using this we can now tailor the correlation properties of the input Gaussian process, through the methods described in the introduction, to control the correlation function of the output non-Gaussian process.

Correlated exponential and Weibull processes

We now discuss the correlation properties of MNLT generated non-Gaussian processes that provide useful models of clutter, either as a representation of the envelope of the process or of its local power, within the compound model. As a first example we consider the $\nu = 1$ gamma (i.e. negative exponential) distributed variable *y* with the pdf

$$P(y) = \exp(-y) \tag{73}$$

In this case the required MNLT is identified as the solution of

$$\int_{y}^{\infty} \exp(-y')dy' = \frac{1}{\sqrt{2\pi}} \int_{x}^{\infty} \exp\left(-x'^2/2\right)dx \tag{74}$$

or, more compactly,

$$\exp(-y) = \frac{1}{2}\text{erfc}\left(x/\sqrt{2}\right). \tag{75}$$

Thus we see that the mapping

$$y = \log\left(2/\text{erfc}\left(x/\sqrt{2}\right)\right) \tag{76}$$

applied to a Gaussian process will generate an exponentially distributed process. Our general result (70) reduces in this case to

$$\langle y(0)y(t)\rangle = \frac{1}{2\pi}\sum_{n=0}^{\infty}\frac{R_G(t)^n}{2^n n!}\left(\int_{-\infty}^{\infty} dx \exp\left(-x^2/2\right)H_n\left(x/\sqrt{2}\right)\log\left(2\Big/\operatorname{erfc}\left(x/\sqrt{2}\right)\right)\right)^2 ; \qquad (77)$$

Note that, on letting $R_G(t)$ go to zero and taking account of the integral

$$\int_{-\infty}^{\infty}\exp\left(-x^2\right)\log\left(\operatorname{erfc}(x)\right)dx = \sqrt{\pi}\left(\log 2 - 1\right) \qquad (78)$$

we recover the totally decorrelated result $\langle y\rangle^2 = 1$.

The numerical integrations over the Hermite polynomials in (77) present no real problems and reveal that the series is very rapidly convergent. Thus, once we have calculated and stored the first few of these integrals, (70) provides us with a tractable and single valued functional relationship between the correlation functions of the input Gaussian and output negative exponentially distributed processes. This then lets us map the required correlation function of the output process point by point onto that of the corresponding input Gaussian process. Assuming that the latter can be constructed by the Fourier synthesis, we are now able to generate the required correlated, exponentially distributed process by MNLT. Figure 1 shows the mapping from R_G to $R_{\exp}$. It is reassuring to note that, by setting R_G to unity, we recover the fully correlated result $\langle y^2\rangle = 2$. By allowing R_G to take negative values the MNLT can generate an exponentially distributed process whose correlation function takes values that, while they are necessarily greater than zero, are less than the fully de-correlated limit $\langle y\rangle^2 = 1$. It is precisely this type of correlation that Oliver's filtering method cannot reproduce. Figure 2 shows the correlation functions of the input and output processes, the former has been given a simple exponentially damped oscillatory form. Detailed comparison of the two curves shows that the 'undershoot' below the fully de-correlated value is less marked in the output process than it is in the input. Most interestingly, Figure1 and the log log plot in Figure 3 show that, to a very good approximation, a positive correlation in the input process is reproduced unchanged in the correlation in the output exponentially distributed process. A slight deviation from this simple behaviour is noticeable as R_G approaches 1, and is emphasised by the linear continuation of the small R_G behaviour into this region. This observation accounts, in the $\nu = 1$ case, for the invariance under the Gaussian-to-gamma MNLT of the correlation functions studied in earlier work.

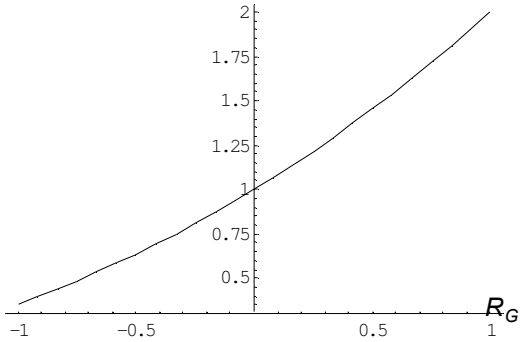

Figure 1: *The mapping between the input and output correlation functions under the MNLT (12)*

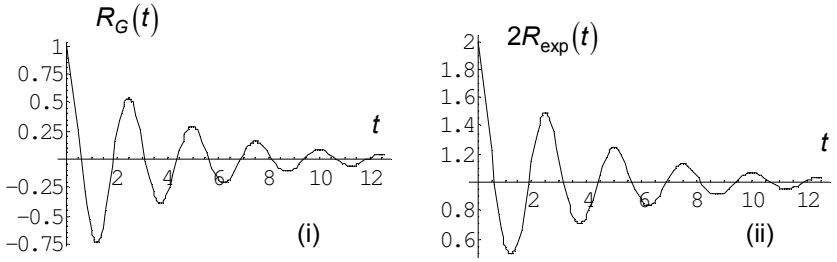

Figure 2*: Input (i) and output (ii) correlation functions displaying oscillatory behaviour*

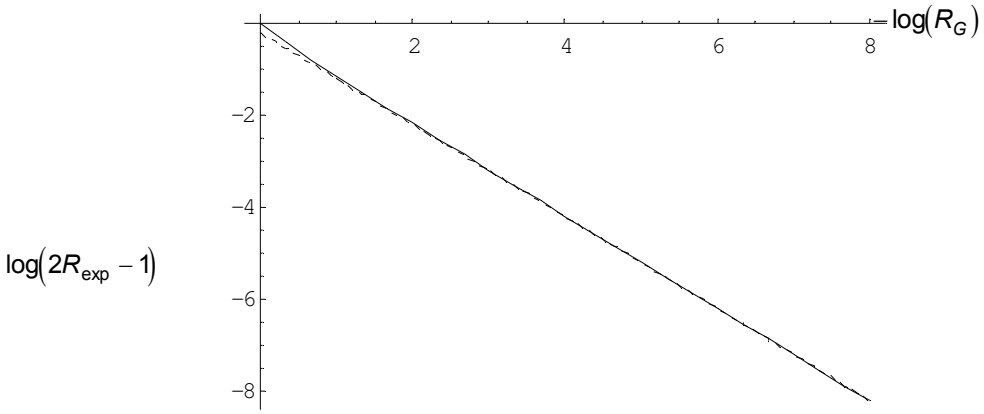

Figure 3: *A log-log plot demonstrating the effective invariance of positive correlation functions under the MNLT (48)*

The Weibull process takes values ξ whose pdf is

$$P_W(\xi) = \alpha b \xi^{\alpha-1} \exp\left(-b\xi^{\alpha}\right); \quad \xi \geq 0$$
$$= 0; \quad \xi < 0 \tag{79}$$

and has been widely used as a model for clutter. We see that the analysis we have just outlined can be applied to the correlation properties of a Weibull process generated by some MNLT. The required MNLT is defined by the equation (we can set *b* equal to unity, without any real loss of generality)

$$\exp\left(-\xi^{\alpha}\right) = \frac{1}{2}\operatorname{erfc}\left(x/\sqrt{2}\right) \tag{80}$$

or

$$\xi = \left(\log\left(2/\operatorname{erfc}\left(x/\sqrt{2}\right)\right)\right)^{\frac{1}{\alpha}}. \tag{81}$$

The correlation in the input Gaussian process is mapped over into the correlation in the MNLT generated Weibull process by

$$\left\langle \xi(0)\xi(t)\right\rangle = \frac{1}{2\pi}\sum_{n=0}^{\infty}\frac{R_G(t)^n}{2^n n!}\left(\int_{-\infty}^{\infty} dx \exp\left(-x^2/2\right)H_n\left(x/\sqrt{2}\right)\left(\log\left(2/\operatorname{erfc}\left(x/\sqrt{2}\right)\right)\right)^{\frac{1}{\alpha}}\right)^2 \tag{82}$$

that can be evaluated by dint of some straightforward numerical integrations. Once this has been done, and the mapping between $\left\langle \xi(0)\xi(t)\right\rangle$ and $R_G(t)$ has been inverted, Weibull distributed noise with a prescribed correlation function can be generated. Figure 4 shows a set of log-log plots analogous to those in Figure 3, and reveals the extent to which the correlation function is preserved in this Weibull case. As the Weibull process becomes progressively more non-Gaussian we see that deviations from a simple linear relation between the input and output correlation functions become increasingly more marked for values of R_G close to unity.

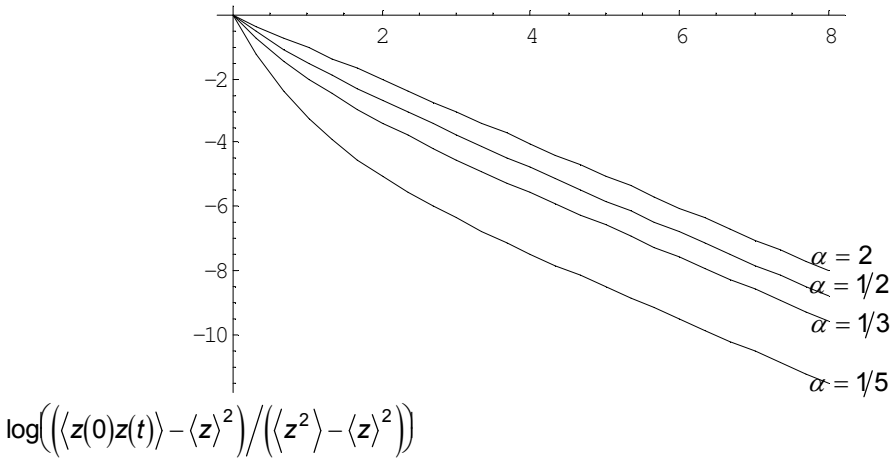

Figure 4: *A log-log plot demonstrating the effect of increasingly non-Gaussian statistics on the mapping of the correlation function under the Gaussian-Weibull MNLT*

It is useful to compare the simulation of exponential and Weibull processes just discussed with methods based on a complex Gaussian process. These are simpler to implement, but afford us considerably less freedom in the modelling of the correlation properties of the process.

A complex Gaussian process consists of real and imaginary parts *x,y* that are themselves Gaussian processes with zero means and equal (unit) variances; at any one time or place *x,y,* are uncorrelated.

The power

$$z = x^2 + y^2 \tag{84}$$

of the process has a pdf that takes the particularly simple form

$$P(z) = \frac{1}{2}\exp(-z/2), \tag{85}$$

where $\langle x^2 \rangle = \langle y^2 \rangle = 1$, while its correlation function follows directly from the Gaussian factorisation property and the correlations between *x,y*:

$$\begin{aligned} \langle z_1 z_2 \rangle &= \left\langle \left(x_1^2 + y_1^2\right)\left(x_2^2 + y_2^2\right) \right\rangle = 4\langle x^2 \rangle + 4\left(\langle x_1 x_2 \rangle^2 + \langle x_1 y_2 \rangle^2\right) \\ &= 4\left(1 + k_0^2\right) \end{aligned} \tag{86}$$

Thus we see that $\langle z_1 z_2 \rangle$ necessarily takes values between those of $\langle z \rangle^2$ and $\langle z^2 \rangle$; an undershoot in the correlation function below the value of the square of the mean, such as that shown in Figure 2, cannot be modeled through (84).

The exponential form taken by (85) facilitates the transformation of *z* into a process with a Weibull pdf (79); the required MNTL is simply

$$\xi = \left(\frac{z}{2}\right)^{\frac{1}{\alpha}}. \tag{87}$$

To relate the correlation function of the output process to that of the input complex Gaussian process we recall the joint pdf of the *z* process takes the form

$$\begin{aligned} P(z_1, z_2) &= \frac{\exp\left(-(z_1 + z_2)/2\right)}{4} \frac{\exp\left(-k_0^2(t)(z_1 + z_2)/2\left(1 - k_0^2\right)\right)}{\left(1 - k_0^2(t)\right)} I_0\left(k_0(t)\sqrt{z_1 z_2}/\left(1 - k_0^2(t)\right)\right) \\ &= \frac{\exp\left(-(z_1 + z_2)/2\right)}{4} \sum_{n=0}^{\infty} L_n(z_1/2) L_n(z_2/2) k_0^{2n}(t) \end{aligned} \tag{88}$$

The expansion is quite analogous to (68): the L_n are Laguerre polynomials defined as a special case ($\alpha = 0$) of

$$L_n^{\alpha}(z) = \frac{\exp(z)}{z^{\alpha} n!} \frac{d^n}{dz^n}\left(z^{n+\alpha} \exp(-z)\right) \tag{89}$$

These encode the factorisation properties of the underlying Gaussian process, in much the same way that the Hermite polynomials do in (68).

Arguments analogous to those leading to (82) show that the correlation function of the Weibull variable (87) can be expressed as

$$\begin{aligned}\left\langle \xi(0)\xi(t)\right\rangle &= \left(\frac{1}{2}\right)^{\frac{2}{\alpha}} \iint dz_1 dz_2 (z_1 z_2)^{\frac{1}{\alpha}} P(z_1, z_2) \\ &= \sum_{n=0}^{\infty} k_0^{2n}(t) \left(\int_0^{\infty} dz z^{\frac{1}{\alpha}} \exp(-z) L_n(z) \right)^2 \end{aligned} \tag{90}$$

The integral over the Laguerre polynomial can be deduced from (89) to be

$$\int_0^{\infty} dz z^{\frac{1}{\alpha}} \exp(-z) L_n(z) = \Gamma(1+1/\alpha) \frac{(-1/\alpha)_n}{n!}; \tag{91}$$

on bringing these results together we find that

$$\left\langle \xi(0)\xi(t)\right\rangle = \Gamma(1+1/\alpha)^2 \; {}_2F_1\left(-1/\alpha, -1/\alpha; 1; k_0^2(t)\right) \tag{92}$$

where we have identified the hypergeometric function. The result (92) reduces to the expected uncorrelated limit when we set $k_0 = 0$; the fully correlated limit is recovered when we set $k_0 = 1$ and use Gauss' formula for the hypergeometric function of unit argument

$${}_2F_1(-1/\alpha, -1/\alpha; 1; 1) = \frac{\Gamma(1+2/\alpha)}{\Gamma(1+1/\alpha)^2}. \tag{93}$$

Much as in the simpler exponentially distributed case we see that the correlation function of a Weibull process generated from the power of a complex Gaussian process cannot take values less than that of the square of its mean; this constraint is removed when we perform the appropriate MNLT directly on a correlated one dimensional Gaussian process. We also note that this method has been adapted to the generation of coherent Weibull clutter, whose power has the distribution (79) and whose real and imaginary parts are those of

$$\cdot \left(\frac{x^2+y^2}{2}\right)^{\frac{1}{2\alpha}} \frac{x+iy}{\sqrt{x^2+y^2}} \tag{94}$$

Thus, in this case, the power spectrum of the input Gaussian process controls the phase of the output process, exactly as it does that of the input process, and the correlation function of the power of the output process. We should also stress that the process generated through (94) is not a satisfactory model for coherent sea clutter as it does not incorporate the large separation in time and length scales characteristic of the decays in the correlations in the local speckle and underlying modulation processes present in the clutter. We will discuss the modeling of coherent clutter in more detail shortly.

Generation of correlated gamma processes by MNLT

The gamma process plays a central role in the modeling of sea clutter, representing the modulation of the scattering due to the small scale structure of the ocean surface by its more slowly varying large scale structure, which is, in effect, resolved by the radar. Consequently much of the initial practical application of the analysis we have developed so far is expected to be to the generation of correlated gamma distributed time series and random fields.

The *Mathematica* add-on package **`Statistics`Continuous Distributions`** contains functions that generate quantiles for a wide variety of non-Gaussian distributions; in the main, however, these are rather too slow for use in practical simulations. Nonetheless we can use these functions to evaluate the integrals in (15) for the gamma distribution with a selection of shape parameters. The results we obtained reproduced the hoped-for fully correlated and wholly uncorrelated limiting values of the correlation functions and mapped out the relationship between the input and output correlation functions in detail. Some typical results are shown in Figure 5. The corresponding log-log plots, analogous to that shown in Figure 3, are qualitatively very similar to those obtained in the Weibull case. The apparent 'invariance under MNLT' of the correlation functions studied in earlier work can be understood in terms of these results. Deviations from a linear relation between the input and output correlation functions are more pronounced in the extreme non-Gaussian regime; it appears that it is these departures, manifest in the behaviour of the correlation function close to the fully correlated limit, that are captured by the 'rules of thumb' suggested by earlier numerical work. We can now replace these empirically derived rules with unambiguous calculations, that need only be made once for each value of the shape parameter ν and stored for subsequent use. In contrast to these rules of thumb, the full calculations are also applicable to input correlation functions that take negative values and correspond to values of the output correlation function that are less than value of the square of the mean of the output process. It is interesting to note that successively larger numbers of terms are required in (70) as ν becomes smaller and the gamma pdf exhibits progressively more singular behaviour at the origin.

When the shape parameter ν took values significantly greater than unity we found that the series (70) was increasingly dominated by its first two terms, with the consequence that the functional form of the correlation function was barely affected at all by the MNLT. Thus when $\nu = 2$ the first two terms in (70) account for 92% of the output correlation function when $R_G = -1$ and 96% when $R_G = 1$; when $\nu = 4.5$ only about a 1% contribution comes from the third and higher order terms in both the extreme correlated and anti-correlated limits. This observation suggests that the MNLT may tend to the form

$$y = \nu + \sqrt{\nu}x \tag{95}$$

which establishes a process whose mean and mean square values correspond with those of the required gamma distribution and which takes the correlation function over unchanged. Direct evaluation shows, for example, that in the case where $\nu = 10.0$ the linear relationship (95) captures the behaviour of the MNLT for small values of $|x|$ but becomes progressively less satisfactory with increasing $|x| > 1.0$.

$\left(\langle \eta(t)\eta(0)\rangle - \nu^2\right)/\nu$

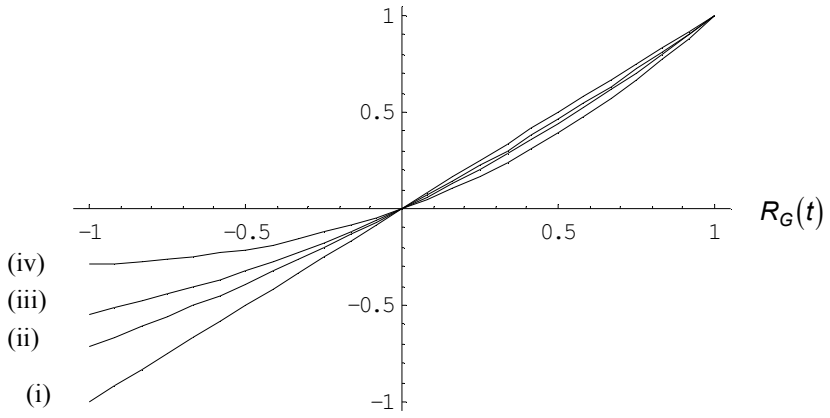

Figure 5: *Correlation functions of MNLT generated gamma processes displayed as functions of the correlation function of the input Gaussian process: (i)* $\nu = \infty$ *, (ii)* $\nu = 1\cdot 3$ *,*
(iii) $\nu = 0\cdot 7$ *,(iv)* $\nu = 0\cdot 3$

We now give a couple of examples of time series and random fields with gamma single point statistics and controlled correlation functions. Figures 6 and 7 below show an example of each. Figure 6 is a time series with ν=0.3, a mean amplitude of 1, and a correlation function given by

$$\langle \eta(0)\eta(t)\rangle = 1 + \frac{\exp\left(-t/10\right)\cos\left(t/8\right)}{\nu}. \tag{96}$$

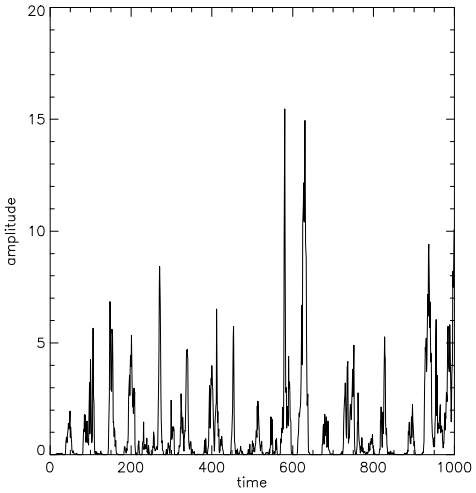

Figure 6: *An amplitude time series of a Gamma process with* ν*=0.3 and a correlation function given by equation (68)*

Figure 7 in a random field of extent 128 in both x and y, with ν=5 and a correlation function given by

$$\langle \eta(0,0)\eta(x,y)\rangle = 1 + \frac{\exp\left(-\frac{x+y}{10}\right)\cos\left(\frac{\pi y}{8}\right)}{\nu}. \tag{97}$$

Both examples are chosen to have the property of the correlation function falling below the mean value squared. This shows in the periodic fluctuations in the simulations and is not accessible with other methods of simulation.

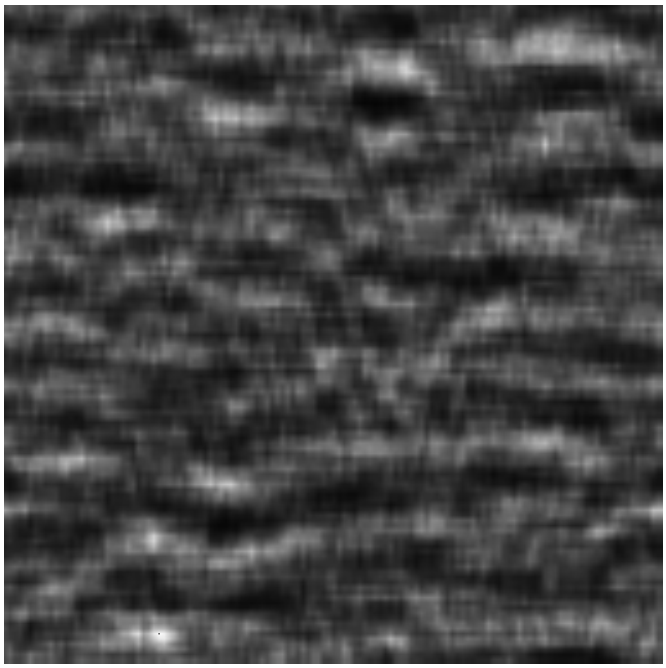

Figure 7: *A Gamma distributed random field with ν=5 and a correlation function given in equation (69)*

Finally we discuss briefly how coherent sea clutter can be simulated; we find that the compound representation allows us to reproduce the salient features of its behaviour much better than can other methods described in the literature.

Figure 8 shows the variation with range of the Doppler spectrum of high-resolution coherent sea clutter; its modulation by the partially resolved large-scale structure of the sea is clearly evident. The basis of the coherent model is a complex Gaussian process whose correlation properties are related to its power (Doppler) spectrum by the Weiner-Khintchine theorem. As we mentioned earlier it has been suggested that non-Gaussian coherent sea clutter might be modeled by subjecting such a complex Gaussian process $x + iy$ to a non-linear transformation that imposes the required single point statistics.

It is possible to tailor the correlation properties of the input complex Gaussian to match those required of the output Weibull process reasonably well , provided the acf does not take values less than the fully de-correlated limit.. However, both the input and output processes in this scheme are stationary; the Weibull clutter does not exhibit the ‘breathing’ modulation seen in the results in Figure 8.

Figure 8: *A range-Doppler-intensity plot of radar sea clutter taken with a 10 GHz radar at vertical polarisation from a clifftop site on the south coast of England at a range of 10 km. The vertical axis is range, sampled at 1.5m intervals over 750m. The horizontal axis is Doppler frequency, from 0 to 250 Hz.*

The compound representation of the non-Gaussian clutter process allows us to remedy this defect quite straightforwardly. Rather than subjecting the complex Gaussian process itself to a non-linear transformation, we multiply it by a correlated gamma process, generated by the method we have just discussed. This product will automatically have K distributed envelope statistics; the slowly varying gamma process imposes the 'non-stationary' breathing modulation while the relatively high frequency structure of the clutter, revealed in the Doppler spectrum, can be modelled through the spectrum assigned to the complex Gaussian process. In fact, by allowing this latter spectrum to depend on the current value of the gamma variate and the values of the shape parameter α and mean clutter power to vary with range, direction and environmental conditions, a very realistic coherent clutter simulation can be developed

The difference between the two methods is illustrated qualitatively in figure 9, which shows the Doppler spectra of simulated clutter as a function of range. Results obtained coherent K distributed clutter, simulated using the compound method, are shown on the left; those for coherent Weibull is simulated using the direct non-linear transformation on the right. The point amplitude statistics have been chosen to be identical (by setting $\alpha = 1/2$ and $\beta = 1$) and the average power spectra are approximately the same. The non-stationary behaviour in the image on the left and the stationary behaviour in that on the right are clearly evident.

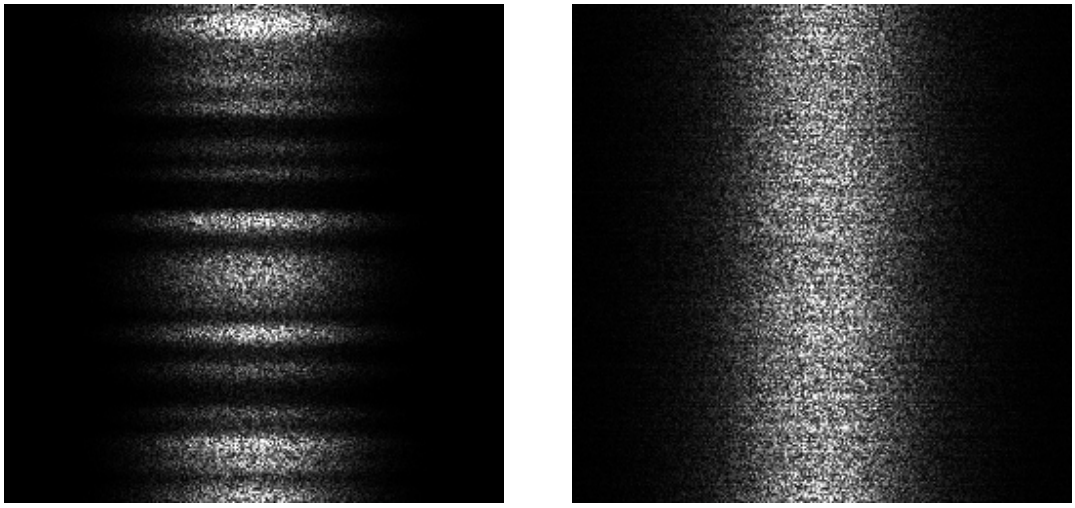

Figure 9: *Coherent non-Gaussian clutter spectral time series. The left image was generated using the compound method and the right using the direct non-linear transformation of a complex Gaussian. The horizontal axes are frequency and the vertical axes are range.*

Exercises

A significant part of any simulation is the generation, presentation and discussion of numerical output. Some of the following exercises will require you to do this; use your favorite software to put forth graphical or tabular results that can form the basis of subsequent discussion. Other exercises have you fill in analytical details that have been glossed over in the session.

1. Simple Brownian motion has provided us with a physical motivation for quite a lot of our discussion of the simulation of correlated Gaussian processes. Simulate the following and present them graphically:

   a) The path of a diffusing Brownian particle

   b) The displacement from the origin of an over-damped Brownian harmonic oscillator.

   c) The complex Ornstein Uhlenbeck process model for coherent clutter

   Look at the power spectra of the processes generated in (b) and (c); what can you say about the results you obtain?

2. Using a time domain technique similar to that described in the session, simulate a correlated Gaussian random variable with the power spectrum

$$S(\omega) = \frac{\omega^2}{\left(\omega^2 + \omega_1^2\right)\left(\omega^2 + \omega_2^2\right)\left(\omega^2 + \omega_3^2\right)}$$

   What is the form taken by the correlation function of this process? Verify the analogue of (41) arising in this problem. Using Mathematica to ease the algebraic load, look at the $\mathbf{AB} + \mathbf{BA}^T = -\mathbf{G}$ "fluctuation-dissipation" result in this case, much as was outlined for the four relaxation time problem in the notes.

3 Simulate correlated Gaussian random processes with a variety of power spectra (choose your own) using the Fourier synthesis method. Examine the output in each case; can you discern any qualitative relationship between the form of the power spectrum and the behaviour of the process as a function of time?

4 The 'hard-limited' signal derived from a correlated Gaussian input takes the value +1 when this is positive and –1 when it is negative. Can you relate the correlation function of the hard-limited signal to that of the underlying Gaussian process? You might want to do this in two ways: directly from the joint pdf of the correlated Gaussian random variables and via the expansion in Hermite polynomials. With any luck you should get the same answer in each case. The paper by Tough and Ward *J. Phys. D*, **32**, 3075, 1999, discusses this and other aspects of the generation of correlated non-Gaussian noise by MNLT in some detail. (The result derived in this exercise is due to Nobel Laureate J.H. van Vleck and greatly facilitated the analysis of correlation functions, which were much easier to measure for hard-limited signals in the old days. The 'Malvern Correlator' also exploited this trick.)

5 Implement a MNLT for generating gamma distributed noise from a Gaussian noise input. Assign a correlation function to the gamma process and evaluate that of the corresponding input Gaussian process. Fourier transform this to obtain its power spectrum. (Do you ever find that this is negative?!!) Generate a bit of correlated gamma noise. Use this to generate the intensity and I and Q components of coherent clutter. Try popping a signal into the clutter and see what it looks like.